Am J Physiol Lung Cell Mol Physiol 318: L135–L146, 2020.
First published November 6, 2019; doi:10.1152/ajplung.00084.2019.

RESEARCH ARTICLE

TRPV4 channel mediates adventitial fibroblast activation and adventitial remodeling in pulmonary hypertension

Laure-Anne Cussac,[1,2]* Guillaume Cardouat,[1,2]* Nichiren Tiruchellvam Pillai,[1,2] Marilyne Campagnac,[1,2] Paul Robillard,[1,2] Anaïs Montillaud,[1,2] Christelle Guibert,[1,2] Philippe Gailly,[3] Roger Marthan,[1,2] Jean-François Quignard,[1,2] Jean-Pierre Savineau,[1,2] and Thomas Ducret[1,2]

[1]*Université de Bordeaux, Centre de Recherche Cardio-Thoracique de Bordeaux, Pessac, France;* [2]*INSERM U1045, Centre de Recherche Cardio-Thoracique de Bordeaux, Bordeaux, France; and* [3]*Laboratory of Cell Physiology, Institute of Neuroscience, Université catholique de Louvain, Brussels, Belgium*

Submitted 21 February 2019; accepted in final form 1 November 2019

Cussac LA, Cardouat G, Pillai NT, Campagnac M, Robillard P, Montillaud A, Guibert C, Gailly P, Marthan R, Quignard JF, Savineau JP, Ducret T. TRPV4 channel mediates adventitial fibroblast activation and adventitial remodeling in pulmonary hypertension. *Am J Physiol Lung Cell Mol Physiol* 318: L135–L146, 2020. First published November 6, 2019; doi:10.1152/ajplung.00084.2019.—Pulmonary arterial adventitial fibroblasts (PAF), the most abundant cellular constituent of adventitia, act as a key regulator of pulmonary vascular wall structure and function from the outside-in. Previous studies indicate that transient receptor potential vanilloid 4 (TRPV4) channel plays an important role in the development of pulmonary hypertension (PH), but no attention has been given so far to its role in adventitial remodeling. In this study, we thus investigated TRPV4 implication in PAF activation occurring in PH. First, we isolated and cultured PAF from rat adventitial intrapulmonary artery. RT-PCR, Western blot, immunostaining, and calcium imaging (fluo-4/AM) showed that PAF express functional TRPV4 channels. In extension of these results, using pharmacological and siRNA approaches, we demonstrated TRPV4 involvement in PAF proliferation (BrdU incorporation) and migration (wound-healing assay). Then, Western blot experiments revealed that TRPV4 activation upregulates the expression of extracellular matrix protein synthesis (collagen type I and fibronectin). Finally, we explored the role of TRPV4 in the adventitial remodeling occurring in PH. By means of Western blot, we determined that TRPV4 protein expression was upregulated in adventitia from chronically hypoxic and monocrotaline rats, two animal models of PH. Furthermore, morphometric analysis indicated that adventitial remodeling is attenuated in PH-induced *trpv4*$^{-/-}$ mice. These data support the concept that PAF play an essential role in hypertensive pulmonary vascular remodeling and point out the participation of TRPV4 channel activity in PAF activation leading to excessive adventitial remodeling.

adventitia; fibroblast; migration; proliferation; pulmonary artery; TRP channel; *trpv4*$^{-/-}$ mouse

INTRODUCTION

Pulmonary hypertension (PH) is a hemodynamic disorder characterized by a progressive elevation of pulmonary arterial pressure leading to right heart failure and, ultimately, to death. From a pathophysiological point of view, PH is a multifactorial disease due to a progressive increase in pulmonary vascular resistance caused, among others, by pulmonary vasculature remodeling, vasoconstriction, and thrombosis (18). The process of pulmonary arterial wall remodeling occurs in the three-layered structure of the vessel (i.e., intima, media, and adventitia) and involves all of the main cell types (i.e., endothelial cells, smooth muscle cells, and fibroblasts, respectively). However, although the adventitia is known to play a key role in the regulation of vascular function and structure (43), little attention has been given so far to the role of the adventitia in the remodeling process occurring during PH.

Remodeled vessels in PH are characterized by adventitial thickening and increased stiffness involving pulmonary artery adventitial fibroblasts (PAF) and connective tissue deposition. Indeed, during the remodeling process, proliferative, migratory, and fibrotic activities of PAF increase (3, 19, 31, 47). Moreover, these cellular responses are strongly enhanced under hypoxic conditions (11), occurring in a variety of chronic lung diseases (chronic obstructive pulmonary disease, asthma. . .), eventually leading to PH of group 3 (12).

At the cellular level, a key step in the initiation of these processes is an increase in $[Ca^{2+}]_i$, which results from a release of intracellular stored Ca^{2+} and/or an influx of extracellular Ca^{2+}, occurring through plasma membrane channels with distinctive Ca^{2+} selectivity. In examining the role of ion channels in PH, we and others recently demonstrated that the activity of transient receptor potential vanilloid 4 (TRPV4) plasma membrane channel was increased in pulmonary artery smooth muscle cells (PASMC) from chronically hypoxic (CH) rat (4, 50), an animal model of PH. Moreover, we previously showed that TRPV4 induces PASMC migration (23, 30). TRPV4 is a subclass of the TRP channel superfamily. It is a Ca^{2+}-permeable nonselective cationic channel, activated by a wide variety of stimuli, including physical, thermal, and chemical stimuli such as the arachidonic acid metabolite epoxyeicosatrienoic acid and the synthetic agonist GSK-1016790A, in particular (45, 48). Importantly, numerous studies showed an emerging role of TRPV4 in mechanical lung injury (15, 26, 29) and progression of myocardial and pulmonary fibrosis (51).

In the present study, we initially found that functional TRPV4 channel is expressed in cultured rat PAF. Since PAF

* L. A. Cussac and G. Cardouat contributed equally to this work.

Address for reprint requests and other correspondence: T. Ducret, Centre de Recherche Cardio-Thoracique de Bordeaux, INSERM U1045, Plateforme Technologique d'Innovation Biomédicale, Hôpital Xavier Arnozan, Avenue du Haut Lévêque, F-33604 Pessac Cedex, France (e-mail: thomas.ducret@u-bordeaux.fr).

represent the most abundant cell type in adventitia and play a central role in the remodeling of this tunica, using genetic (siRNA) or pharmacological inhibition, we then determined that TRPV4 plays a key role in proliferation, migration, and synthesis of extracellular matrix, which are key cellular elements in the pathogenesis of PH. Moreover, TRPV4 was upregulated in pulmonary artery adventitial layer from monocrotaline (MCT) and CH rats, two models of PH corresponding to the first (pulmonary arterial hypertension, including idiopathic PH) and the third groups of PH (due to lung disease or chronic hypoxemia), respectively (42). Finally, the associated adventitial remodeling was significantly attenuated in CH and MCT *trpv4*$^{-/-}$ mice.

MATERIALS AND METHODS

Animal model. The investigation was carried out according to the animal care and use of our local ethics committee ("Comité d'éthique de Bordeaux en expérimentation animale"; protocol number: APAFIS no. 9212–2017031018562273v5) in agreement with the *Guide for the Care and Use of Laboratory Animals* published by the US National Institutes of Health and European directives. Experiments were conducted on Wistar male rats (200–300 g) or C57BL/6J male *trpv4*$^{-/-}$ and *trpv4*$^{+/+}$ mice (20–25 g). The *trpv4*$^{-/-}$ mice were generated by targeted deletion of exon 12 of the *trpv4* gene (22) and backcrossed on a C57BL/6J background before starting the study (37). For in vitro and histology experiments, rats and mice were euthanized by intraperitoneal injection of pentobarbital sodium (120 mg/kg). To measure right ventricle pressure, mice were anesthetized by intraperitoneal injection of ketamine (100 mg/kg) and xylazine (10 mg/kg) and then euthanized.

PAF isolation and culture. Intrapulmonary arteries (IPA) of the first order from lungs of normoxic rats were dissected under binocular control and sterile conditions. Adventitia was removed, cut in several pieces (2 mm^2), and seeded in Petri dishes. Explants were cultured 10–14 days in culture medium (DMEM-HEPES supplemented with 1% penicillin-streptomycin, 1% Na-pyruvate, and 1% nonessential amino acids) enriched with 20% fetal calf serum (FCS) at 37°C in a humidified atmosphere gassed with 5% CO_2. PAF were then passaged and cultured in medium containing 10% FCS. Cells of the 2–3 passages were used in the experiments. Typical morphologic appearance of fibroblasts was confirmed by positive immunostaining for vimentin (clone V9, 1/500, Sigma) and negative staining for von Willebrand factor (AB7356, 1/500, Millipore), calponin (SC-58707, 1/500, Santa Cruz), and α-smooth muscle actin (clone 1A4, 1/500, Sigma) (Fig. 1). For control immunostaining, rat PASMC and human pulmonary arterial endothelial cells were used. Rat PASMC were obtained as previously described (9). Human pulmonary arterial endothelial cells were purchased from PromoCell.

Short interfering RNA knockdown of TRPV4. For transient transfections, a scrambled control oligonucleotide (AllStars Negative Control siRNA, Qiagen) or a mix of two different TRPV4 short interfering (si)RNA (FlexiTube siRNA SI00267743 and SI00267750, Qiagen) were used at a final concentration of 25 nM. Forty-eight hours before the experiments, PAF were transfected using HiPerFect Transfection Reagent according to the manufacturer's instructions (Qiagen).

RNA and cDNA synthesis. RNA was extracted using RNeasy Plus Micro Kit (Qiagen) according to the manufacturer's instructions. The concentration of RNA was measured spectrophotometrically by SPECTROstar Nano absorbance microplate reader (BMG LABTECH). The total RNA (500 ng) was reverse transcribed into cDNA by using qScript cDNA SuperMix Kit (Quantabio) at 42°C for 30 min followed by heating at 85°C for 5 min to inactivate reverse transcriptase.

Polymerase Chain Reaction. PCR was performed with a Bio-Rad CFX96. cDNA from 5 ng of total RNA were added to 5 μL of Perfect SYBR Green Supermix (Quantabio) and 2.5 μL of each of the appropriate primers (Sigma, see Table 1 for concentrations and sequences). The reaction was initiated at 95°C for 2 min, and followed by 40 cycles of denaturation at 95°C for 10 s and annealing/extension at 60°C for 30 s. PCR negative controls were systematically made by using water instead of cDNA. All specific primers were designed by using the primer analysis software (NCBI Primer-BLAST). The efficiency of the PCR reactions was always around 100%. Specificity of the amplified PCR products was checked with melting curve analysis and by electrophoresis analysis on a 2% agarose gel containing SYBR Green.

Western blot. Western blot experiments were conducted on IPA adventitia or cultured PAF. After removal, adventitia was crushed and homogenized using a mortar and pestle and lysis buffer containing 160 mM Tris·HCl (pH 6.3), 5% sodium dodecyl sulfate, and antiprotease cocktail (Sigma). Cultured cells were scraped and incubated in 70 μL of RIPA lysis buffer system supplemented with protease inhibitor cocktail (1/100), orthovanadate sodium (1/100), and PMSF (1/100) (ChemCruz) for 30 min on ice. Insoluble material was then removed by centrifugation at 15,000 *g* for 10 min at 4°C, and the amount of proteins was assessed by the Lowry method. After heat denaturation, 30 μg of proteins was separated by 4–20% acrylamide gel electrophoresis. The proteins were then transferred onto nitrocellulose membranes using Trans-Blot Turbo Transfer System. After saturation for 1 h using 0.1% TBS-TWEEN and 5% nonfat milk, membranes were incubated overnight at 4°C with primary antibodies: anti-TRPV4 (AB191580, 1/1,000, Abcam), anti-fibronectin (AB2413, 1/1,000, Abcam), anti-collagen type I (ABT123, 1/1,000, Millipore), or anti-GAPDH (SC25778, 1/1,000, Santa Cruz). The membranes were then treated with the corresponding horseradish peroxidase-linked secondary antibodies (Pl1000, 1/10,000, Vector) for 1 h at room temperature. Membranes were processed for chemiluminescent detection using horseradish peroxidase substrate (Millipore), according to the manufacturer's instructions. Immunoblots were then revealed and acquired using a Bio-Rad ChemiDoc XRS+ System. Images were quantified using Image Laboratory software (Bio-Rad).

TRPV4 immunostaining in living cells. PAF seeded on glass coverslips were washed with ice-cold phosphate-buffered saline (PBS). Unspecific binding sites were blocked with PBS containing 1.5% bovine serum albumin (BSA) for 45 min at 4°C. A polyclonal anti-TRPV4 extracellular antibody (ACC-124, 1/100, Alomone) with or without the corresponding blocking peptide in PBS 1.5% BSA was applied 45 min at 4°C. Cells were then washed with PBS and labeled with Alexa-Fluor488 secondary antibody (A11008, 1/200, Invitrogen) for 45 min at 4°C in PBS 1.5% BSA. PAF were then fixed for 10 min in 4% paraformaldehyde solution and cell nuclei were stained with DAPI for 5 min (5 μg/mL, Sigma). Slides were mounted with coverslips and then observed under a Nikon D-Eclipse C1 confocal scanning microscope using a Nikon Apo Plan ×60/1.4 NA oil immersion objective.

Real-time Ca^{2+} fluorescence confocal imaging. In real-time fluorescence imaging, the fluo-4/AM probe was used for measuring variations in the $[Ca^{2+}]_i$. PAF were bathed in physiological saline solution (in mM: 130 NaCl, 5.6 KCl, 2 $CaCl_2$, 1 $MgCl_2$, 11 glucose, 8 HEPES, pH = 7.4) and incubated with fluo-4/AM (1 μM, Invitrogen) during 30 min at constant air-conditioned room temperature. After extensive wash, fluorescence was observed under a Nikon D-Eclipse C1 confocal scanning microscope (excitation wavelength 488 nm; emitted fluorescence recorded at 500–530 nm). Images were acquired during 10 min at a frequency of 0.125 Hz. The inhibitor and the siRNA were added in the medium 0.5 and 48 h, respectively, before the measurements. The amplitude of the calcium rise was determined as the maximum $\Delta(F/F_0)$ reached during the recording time, i.e., between 4 and 472 s after GSK1016790A application depending on the cells. A calcium response was considered positive when $\Delta(F/F_0)$ was ≥ 0.1.

Cell population doubling time determination. An automated cell counter was used to determine the cell population doubling time of the

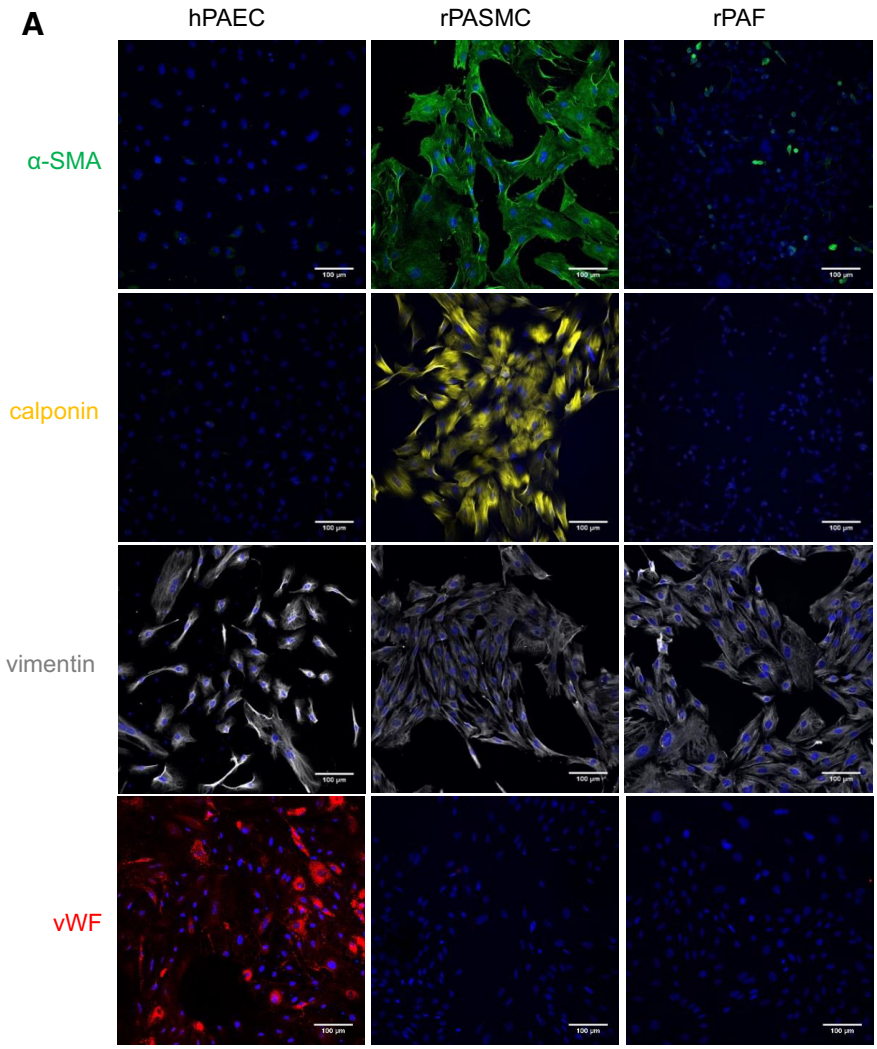

B

	hPAEC	rPASMC	rPAF
α-Smooth Muscle Actin (α-SMA)	✘	✓	✘
calponin	✘	✓	✘
vimentin	✓	✓	✓
von Willebrand factor (vWF)	✓	✘	✘

Fig. 1. Phenotyping of cultured rat pulmonary arterial adventitial fibroblasts. *A*: representative confocal immunofluorescence fields of human pulmonary arterial endothelial cells (hPAEC), rat pulmonary arterial smooth muscle cells (rPASMC), and rat pulmonary arterial adventitial fibroblasts (rPAF). Cells were stained with a primary antibody for α-smooth muscle actin (α-SMA), calponin, vimentin, or von Willebrand factor (vWF). All images were taken with the same illumination time. Scale bar = 100 μm. *B*: summary table of the immunostainings obtained in the 3 different cell types.

cultured PAF. Cells were seeded in a 24-well tissue culture plate and cultured in complete culture medium containing 10% FCS. At regular time intervals (6, 12, and 24 h), cells were detached with trypsin and the total number of cells was counted with a Logos Biosystems LUNA Automated Cell Counter.

In vitro proliferation assay. Cells were seeded in a 96-well tissue culture plate and cultured in complete culture medium containing 10% FCS. After 24 h, the medium was removed and replaced by a serum-free medium. After an additional period of 12 h, cells were incubated with BrdU (10 μM) in the same medium containing or not the agonist (GSK1016790A, Sigma), the inhibitor (HC067047, Sigma), or the siRNA. After incubation for 24 h, DNA synthesis was then assayed using Cell Proliferation ELISA, BrdU colorimetric method (Roche Applied Science), according to the manufacturer's instructions. Newly synthesized BrdU-DNA was determined using a SPECTROstar Nano absorbance microplate reader (BMG LABTECH) at a wavelength of 380 nm with a reference wavelength of 490 nm. The inhibitor and the siRNA were added in the medium 24 and 48 h respectively, before the measurements.

In vitro migration assay. PAF were seeded in a 12-well tissue culture plate in culture medium with 10% FCS until confluence. After an additional period of 12 h in serum-free culture medium, a straight scratch was performed in the monolayer of cells using a pipette tip to obtain a wide acellular area and cells were incubated in the same medium containing or not the agonist, the inhibitor, or the siRNA. Following 6 h under these conditions, imaging of the two wound

Table 1. *Sequences of the primer pairs*

Gene	Sequence	GenBank Accession Number	Product Length, bp	Product Tm, °C	Concentration, μM
hprt1	S: TGTTGGATATGCCCTTGACTA	NM_012583.2	178	60	5
	AS: AGATGGCCACAGGACTAGAAC				
trpv4	S: GCCATCGCTGACAACACCCGAGA	NM_023970.1	208	60	5
	AS: TGTCCTCATCTGTCACCTCCCGTC				
ywhaz	S: CACAGCGGTAAACAAAATCCCAT	NM_011740.3	173	60	5
	AS: ACATTAAAACAAAGCTAGCCGTCA				

Sense (S) and antisense (AS) are shown as well as GenBank accession number, product length, product melting temperature (Tm), and concentration for *hprt1* (hypoxanthine guanine phosphoribosyl transferase 1), *trpv4*, and *ywhaz* (tyrosine 3-monooxygenase/tryptophan 5-monooxygenase activation protein zeta) genes.

edges was performed (at three different positions along the scratch) and cells that migrated into the acellular area were counted under a bright-field VWR microscope. The inhibitor and the siRNA were added in the medium 24 and 48 h, respectively, before the measurements.

Induction of pulmonary hypertension. Animals (mice or rats) were separated into two groups for PH induction. The first group (CH animals) was exposed to chronic hypoxia for 3 wk in a hypobaric chamber (50 kPa). The second group (MCT animals) was intraperitoneally injected with MCT (Sigma): 60 mg/kg body weight for the rats (one single injection, 4 wk before the experiments) or 600 mg/kg for the mice (once weekly for 10 wk) as previously discussed (39). The establishment of the pathology was confirmed as indicated below.

Determination of right ventricular systolic pressure and right heart hypertrophy. Right ventricular systolic pressure (RVSP) was measured in anesthetized open-chest mice by a heparin-filled hypodermic needle inserted in the right ventricle through the cardiac wall and connected to a Baxter Uniflow gauge pressure transducer. After completion of the hemodynamic evaluation, mice were euthanized. The atria, main pulmonary artery, and aorta were dissected from the heart of rats and mice. The right ventricle was separated from the left ventricular wall and septum, and were both weighed. Right ventricular hypertrophy was evaluated as the ratio of the weight of the right ventricle to that of the left ventricle plus the septum (Fulton's index).

Morphometric study of pulmonary arteries. Lungs were fixed in 4% paraformaldehyde solution. Multiple 4 μm transverse slices were

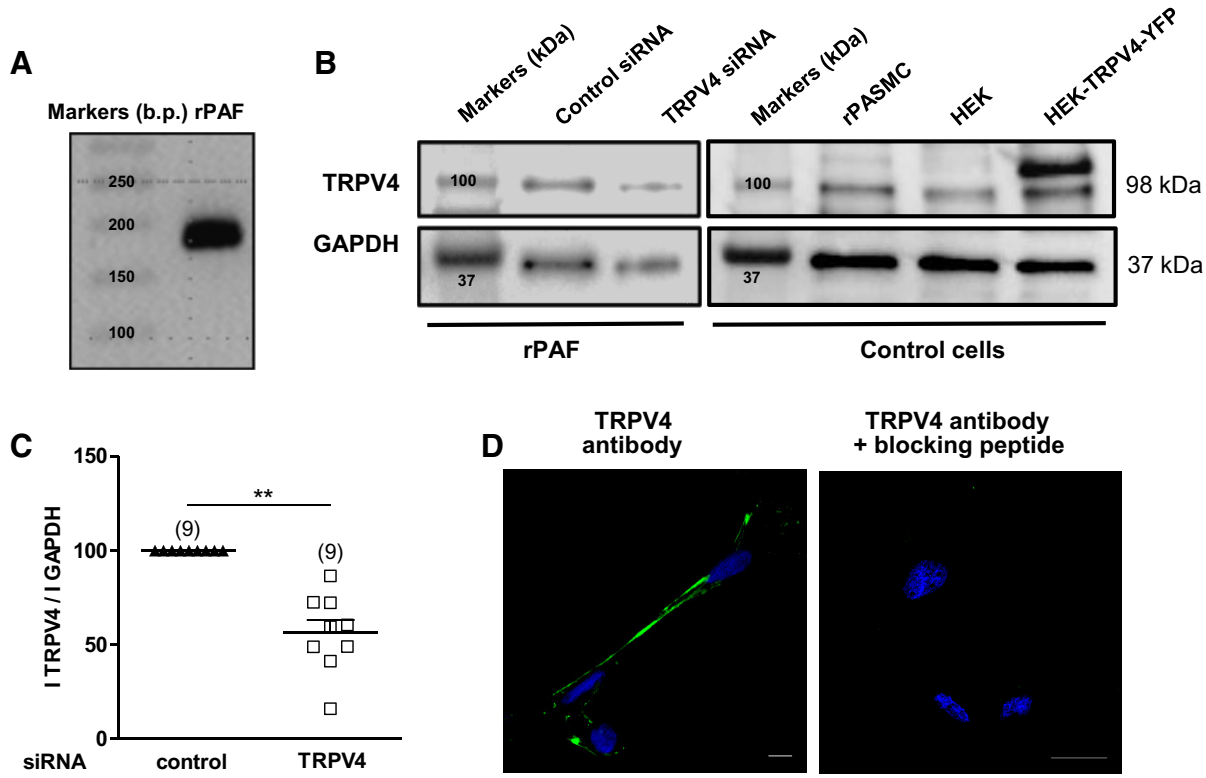

Fig. 2. Expression of transient receptor potential vanilloid 4 (TRPV4) channel in cultured rat pulmonary arterial adventitial fibroblasts. *A*: representative RT-PCR showing the presence of TRPV4 transcript in cultured rat pulmonary arterial adventitial fibroblasts (rPAF). Expected length of PCR products is 208 bp. *B*: representative Western blots showing the presence of TRPV4 protein in cultured rPAF transfected or not with control siRNA or TRPV4 siRNA. Rat pulmonary arterial smooth muscle cells (rPASMC) and HEK293T cells transfected (HEK-TRPV4-YFP) or not (HEK) with *TRPV4-YFP* were used as controls. All samples ran on the same gel. *C*: summary of TRPV4 protein expression in PAF transfected with control siRNA or TRPV4 siRNA measured by Western blot and normalized to GAPDH expression level. *D*: representative confocal immunofluorescence fields of PAF. Cell nuclei were stained with DAPI (blue). Cells were stained with a primary antibody for TRPV4 and an Alexa-Fluor 488-conjugated secondary antibody in absence (*left*) or presence (*right*) of the corresponding blocking peptide. All images were taken with the same illumination time. Scale bar = 20 μm. The number of independent experiments is indicated in parentheses. **Significant difference when $P < 0.01$.

processed in paraffin wax using a Leica Biosystems RM2245 microtome, deparaffinized, and stained with Elastica van Gieson (Elastic Stain kit, Sigma) to detect elastic fibers. The sections were observed by bright-field microscopy using a Hamamatsu NanoZoomer 2.0HT microscope. Areas of the different tunica were quantified and normalized to the diameter of the vessel (30–150 μm).

TRPV4 immunostaining in transverse sections of pulmonary arteries. IPA were fixed in 10% Formalin (Sigma) solution. Multiple 8 μm transverse slices were processed in Optimal Cutting Temperature mounting medium Q Path (VWR) using a Leica Biosystems CM1950 cryostat. Sections were first incubated in PBS-SDS 1% for 5 min and then in PBS blocking buffer containing 0.05% TBS-TWEEN and 3% BSA for 45 min at room temperature. The primary anti-TRPV4 antibody (Ab191580, 1/100, Abcam) was added overnight at 4°C. Sections were then washed with PBS and incubated with Alexa-Fluor568 secondary antibody (A11011, 1/200, Invitrogen) for 2 h at room temperature. Nuclei were labeled with DAPI for 5 min (5 μg/mL, Sigma). Sections were then observed with a Nikon D-Eclipse C1 confocal scanning microscope.

Data and statistical analysis. Results are expressed as a means ± SE. The number of animals (Figs. 6 and 7), responsive cells (Fig. 3), or independent experiments (Figs. 2, 4, and 5) is indicated in each bar graph figure. Mann-Whitney test was used to determine statistical significance between two groups. One-way ANOVA followed by Newman-Keuls post hoc test was used to compare multiple groups. Differences with $P < 0.05$ were considered significant. Statistical analysis was performed with the Prism 5 software (GraphPad).

RESULTS

Expression and function of TRPV4 in rat PAF. Since PAF are the most abundant cell type in adventitia and play a central role in its remodeling (43), we assessed the functional expression of TRPV4 in cultured rat PAF.

First, we verified the expression of TRPV4 using reverse transcription-PCR technique. PCR product of the expected sizes (208 bp) was obtained (Fig. 2*A*). As shown in Fig. 2*B*, Western blot revealed expression of the protein with the predicted molecular mass (98 kDa). Immunostaining with anti-TRPV4 antibody and the corresponding blocking peptide also revealed that PAF were TRPV4 positive (Fig. 2*D*).

To investigate TRPV4 function, we studied the effect of GSK1016790A, a selective TRPV4 agonist, on $[Ca^{2+}]_i$ in cultured rat PAF. In 81% of tested cells, application of GSK1016790A (100 nM) elicited a fast and sustained increase in $[Ca^{2+}]_i$ (Fig. 3*A*). In the presence of HC067047 (0.1, 1, or 5 μM), a specific inhibitor of TRPV4, the percentage of responding cells and the GSK1016790A-induced $[Ca^{2+}]_i$ rise were strongly reduced (Fig. 3, *B* and *C*), thus confirming that the GSK1016790A-induced calcium response was related to TRPV4 activation. In the same way, although HC067047 TRPV4-dependent specific effect was verified by using very

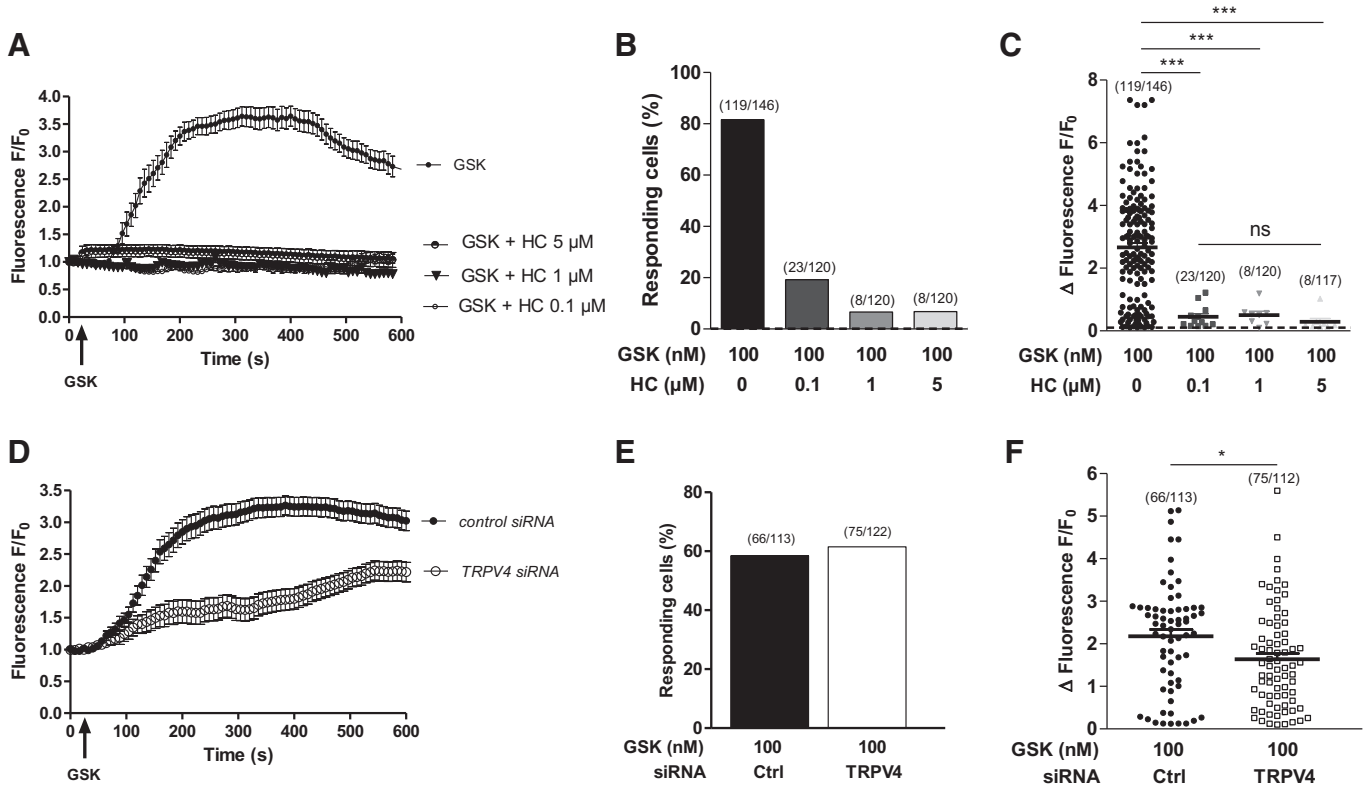

Fig. 3. Functional activity of transient receptor potential vanilloid 4 (TRPV4) channel in cultured rat pulmonary arterial adventitial fibroblasts. *A–C*: variations of relative cytosolic Ca^{2+} concentration were monitored by fluorescence video microscopy in fluo4-loaded pulmonary arterial adventitial fibroblasts (PAF) (*A*). Cells were bathed in physiological saline solution in absence or presence of the specific TRPV4 inhibitor HC067047 (HC; 0.1, 1, and 5 μM). GSK1016790A (GSK, 100 nM), a selective TRPV4 agonist, was added at 16 s (as indicated by the arrow). Results are represented as mean ± SE. Percentages of responding cells (*B*) and amplitude of the calcium rises (*C*) in response to GSK1016790A. *D–F*: variations of relative cytosolic Ca^{2+} concentration in fluo4-loaded PAF transfected with control siRNA or TRPV4 siRNA (*D*). Transfected cells were bathed in physiological saline and GSK1016790A (100 nM) was added at 16 s. Results are represented as mean ± SE. Percentages of responding cells (*E*) and amplitude of the calcium rises (*F*) in response to GSK1016790A. The number of cells (*A–F*) is indicated in parentheses. Significant difference $*P < 0.05$, $***P < 0.001$. ns, no significant difference.

low concentration, i.e., 100 nM, TRPV4 expression was inhibited specifically using siRNA. By Western blot analysis, we could measure a decrease of 44% of the TRPV4 protein expression in cells transfected with TRPV4 siRNA, in comparison with cells transfected with control scrambled siRNA (Fig. 2, *B* and *C*). These transfected PAF were then studied functionally. As expected, we observed that TRPV4 knockdown significantly reduced the GSK1016790A-induced Ca^{2+} response (Fig. 3, *D–F*).

Involvement of TRPV4 in rat PAF proliferation, migration and extracellular matrix synthesis. Since PAF contribute to structural changes in the adventitia and express functional TRPV4 channels allowing $[Ca^{2+}]_i$ increase, we asked the question whether TRPV4 mediate major cellular events underlying vascular remodeling: proliferation and migration.

First, we determined the cell population doubling time of the cultured PAF, which was ~12 h (Fig. 4*A*).

Then, using BrdU colorimetric method, we investigated the implication of TRPV4 in PAF proliferation (Fig. 4, *B* and *C*). As shown in Fig. 4*B*, application of GSK1016790A for 24 h significantly stimulated proliferation (1.25-fold increase). This TRPV4-induced proliferation was dose dependently inhibited by addition of 1 or 5 μM HC067047 (Fig. 4*B*) or TRPV4 siRNA (Fig. 4*C*), confirming that this observed effect was related to TRPV4 activation.

In another set of experiments, we assessed the ability of GSK1016790A to increase PAF migration (Fig. 4, *D* and *E*). To be sure that potentially observed change in cell migration was not due to increased cell growth, cells were incubated with GSK1016790A for 6 h. As determined by wound-healing assay, the agonist significantly stimulated migration by 1.4-fold (Fig. 4*D*). We then confirmed the implication of TRPV4 by pharmacological (HC067047, Fig. 4*D*) or genetic (siRNA, Fig. 4*E*) inhibitions.

Since PAF contribute to the reorganization of the extracellular matrix via matrix deposition, we also assessed whether TRPV4 regulated the expression of collagen type I and fibronectin. Using Western blot experiments, we demonstrated that GSK1016790A upregulates the expression of both proteins by 25 and 41%, respectively (Fig. 5, *A–C*). Notably, this matrix overproduction was abrogated in presence of HC067047 (Fig. 5, *A–C*) or TRPV4 siRNA (Fig. 5, *D–F*). These results suggest that TRPV4 potentiates extracellular matrix deposition by PAF and could thereby modulate the matrix stiffness.

Upregulation of TRPV4 in pulmonary artery adventitia from CH and MCT rats. Since TRPV4 contributes to key cellular elements (proliferation, migration, and upregulation of extracellular matrix proteins) implicated in the pathogenesis of PH, we thus investigated TRPV4 implication in adventitia remodeling occurring in PH. Immunofluorescent labeling studies revealed the presence of TRPV4 in rat pulmonary artery wall (Fig. 6*A*). The auto fluorescence of the external and internal elastic laminae (in green) allowed us to delimit the three-

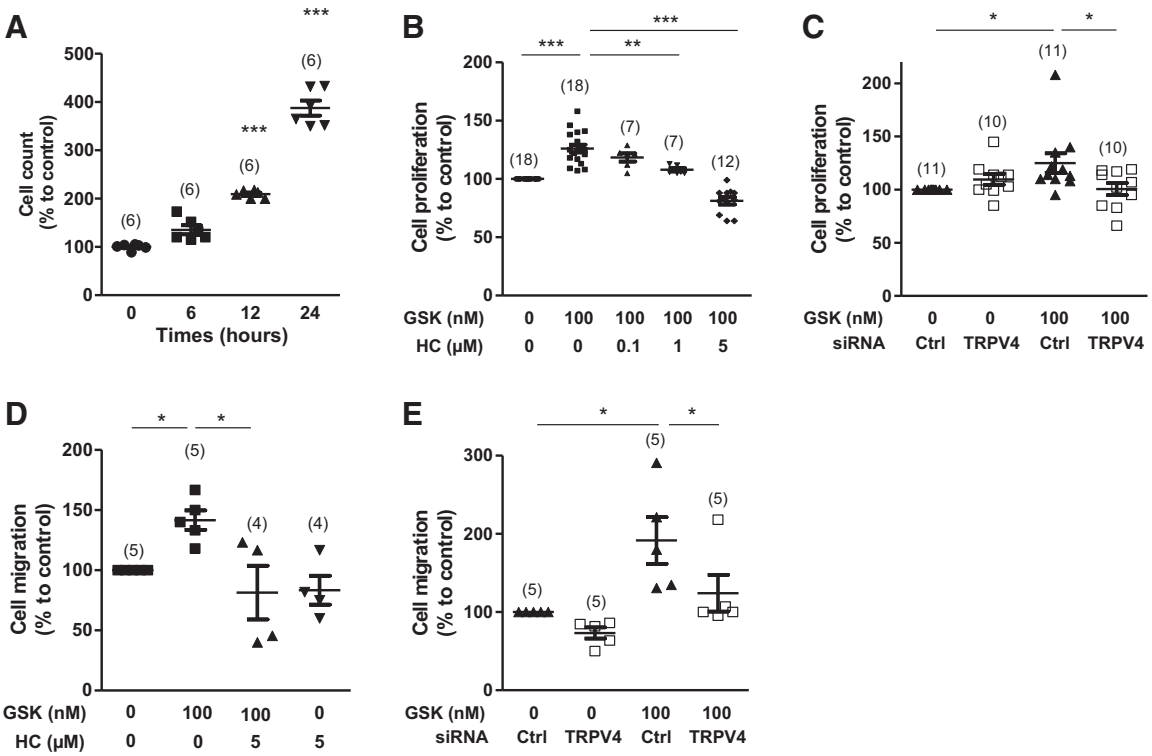

Fig. 4. Involvement of transient receptor potential vanilloid 4 (TRPV4) in cultured rat pulmonary arterial adventitial fibroblast proliferation and migration. *A*: determination of the cell population doubling time of the cultured pulmonary arterial adventitial fibroblasts (PAF). *B* and *C*: effects of GSK1016790A (GSK) on PAF proliferation, assessed by quantitative determination of DNA synthesis using the cell proliferation ELISA BrdU colorimetric method. Cells were incubated with BrdU (10 μM) in serum-free medium containing or not the agonist (GSK, 100 nM), the inhibitor [HC067047 (HC); 0.1–5 μM, *B*], or the siRNA (control and TRPV4, *C*). *D* and *E*: effects of GSK on PAF migration evaluated by wound-healing assay. Cells were incubated in serum-free medium containing or not the agonist (GSK, 100 nM), the inhibitor (HC067047, 5 μM, *D*), or the siRNA (control and TRPV4, *E*). Results are expressed as number of migrating PAF in the acellular area 6 h after wounding related to control conditions. The number of independent experiments is indicated in parentheses. Significant difference $*P < 0.05$, $**P < 0.01$, and $***P < 0.001$.

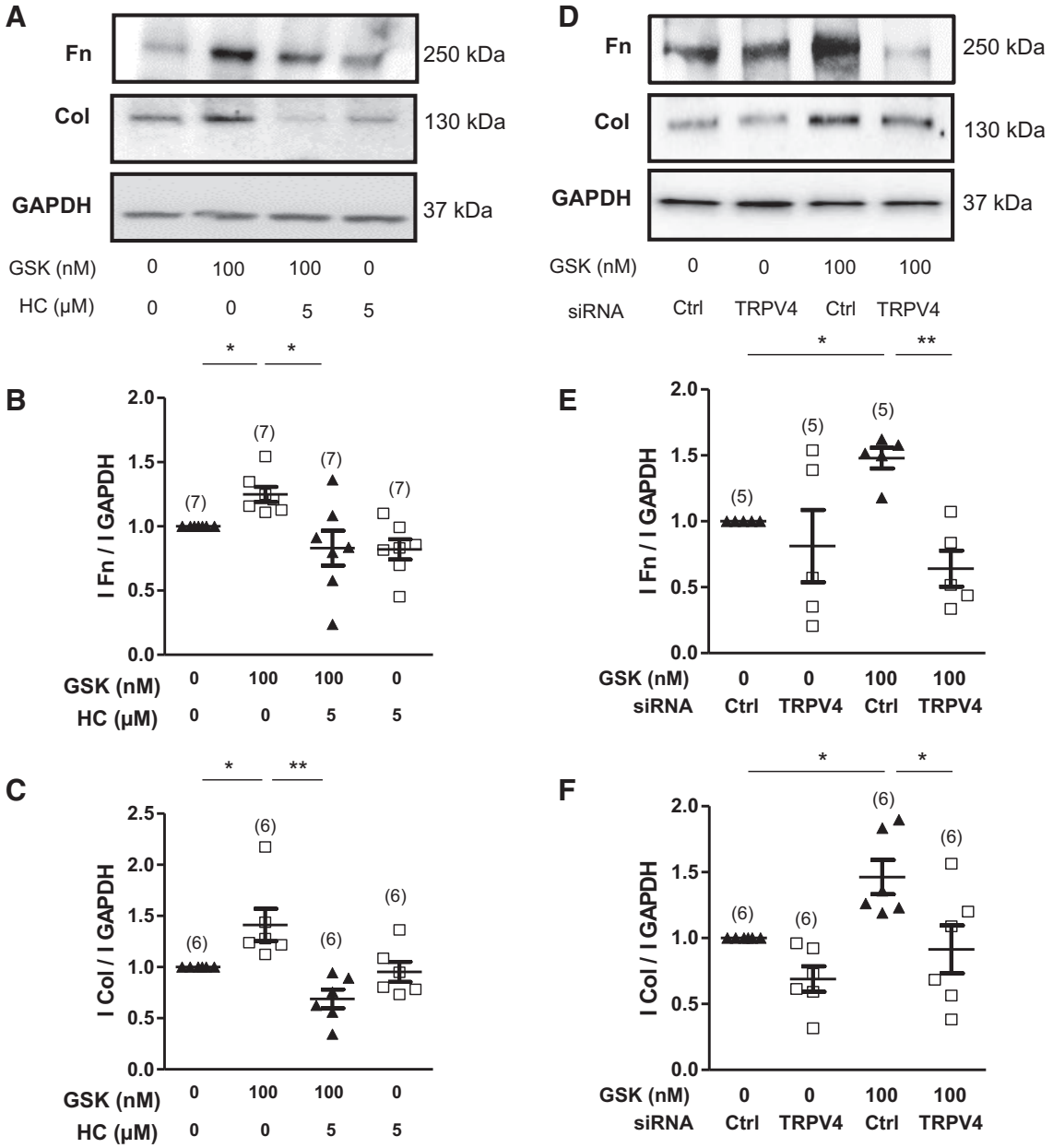

Fig. 5. Involvement of transient receptor potential vanilloid 4 (TRPV4) in expression of fibronectin and collagen type I in cultured rat pulmonary arterial adventitial fibroblasts. *A* and *D*: representative Western blots showing the presence of fibronectin (Fn) and collagen type I (Col) proteins in pulmonary arterial adventitial fibroblasts (PAF) cultured in absence or presence of GSK1016790A (GSK; 100 nM; *A*) or HC067047 (HC; 5 μM) or PAF transfected with control or TRPV4 siRNA (*D*). All samples ran on the same gel. *B*, *C*, *E*, and *F*: summary of Fn (*B* and *E*) and Col (*C* and *F*) protein expressions measured by Western blot and normalized to GAPDH expression level. The number of independent experiments is indicated in parentheses. Significant difference $*P < 0.05$ and $**P < 0.01$.

layered structure of the vessel and to show that TRPV4 was present in the three tunica. In particular, using Western blot experiments, we confirmed the presence of the protein in the adventitia (Fig. 6, *B* and *C*).

Interestingly, a significant increase in protein levels was observed in adventitia from both CH and MCT rats, two different pulmonary hypertensive models, compared with adventitia from control (CTL) rats, by 173 and 108%, respectively (Fig. 6, *A–C*).

Attenuation of adventitial remodeling in PH-induced trpv4$^{-/-}$ mice. In another set of experiments, we used *trpv4*$^{-/-}$ mice. As already reported (50), in CH-induced PH, *trpv4* gene deletion significantly attenuated the increase in Fulton's index and RVSP (Fig. 7*A*). Interestingly, histopathological analysis revealed pronounced vascular remodeling in CH animals (Fig. 7*B*): we observed increased cross-sectional surfaces of the adventitia and the media by 1.6 and 1.4-fold, respectively (Fig. 7*C*). Moreover, CH *trpv4*$^{-/-}$ mice had significantly reduced adventitia and media hypertrophy (by 34 and 32%, respectively) compared with CH *trpv4*$^{+/+}$ mice (Fig. 7*C*). These results were also observed in the MCT-induced mild PH mouse model (39) (data not shown). Indeed, in MCT mice ($n = 7$), adventitial and medial cross-sectional surfaces were increased by 89

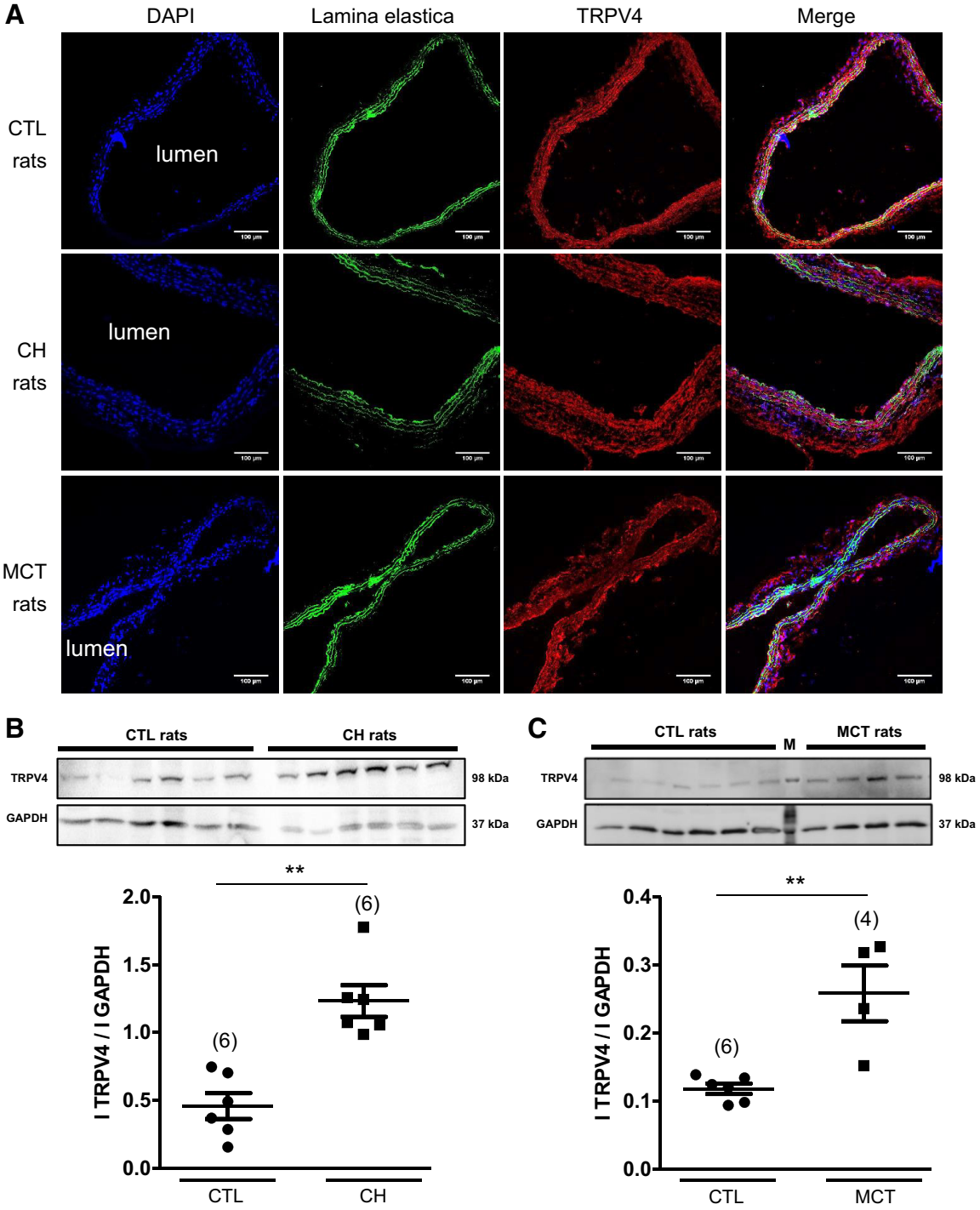

Fig. 6. Transient receptor potential vanilloid 4 (TRPV4) channel expression in rat pulmonary artery adventitia. *A*: representative confocal immunofluorescent labeling experiments in transverse sections of control (CTL), chronically hypoxic (CH), and monocrotaline (MCT) rat pulmonary arteries. The autofluorescence signals of the vessel corresponded to the elastic laminae (green, *2nd column*). Cell nuclei were stained with DAPI (blue, *1st column*). Cells were stained with a primary antibody for TRPV4 and an Alexa-Fluor 568-conjugated secondary antibody (red, *3rd column*). Merging image (*4th column*). Scale bar = 100 μm. *B* and *C*: *top*: representative Western blots showing TRPV4 expression in adventitia from CTL, CH, and MCT rats. All samples ran on the same gel. *Bottom*: summary of TRPV4 protein expression measured by Western blot and normalized to GAPDH expression level in CTL, CH, and MCT rats. M, markers of molecular weight. The number of rats is indicated in parentheses. Significant difference $^{**}P < 0.01$.

and 25%, respectively. A *trpv4* knockout protective effect ($n = 7$) was also observed in this mild PH model, where we noted a significantly reduced adventitia and media hypertrophy by 35% and 20%, respectively.

Taken together, these results are in agreement with precedent ones (46, 50) and show, for the first time, that TRPV4 contributes to the adventitial remodeling occurring in PH.

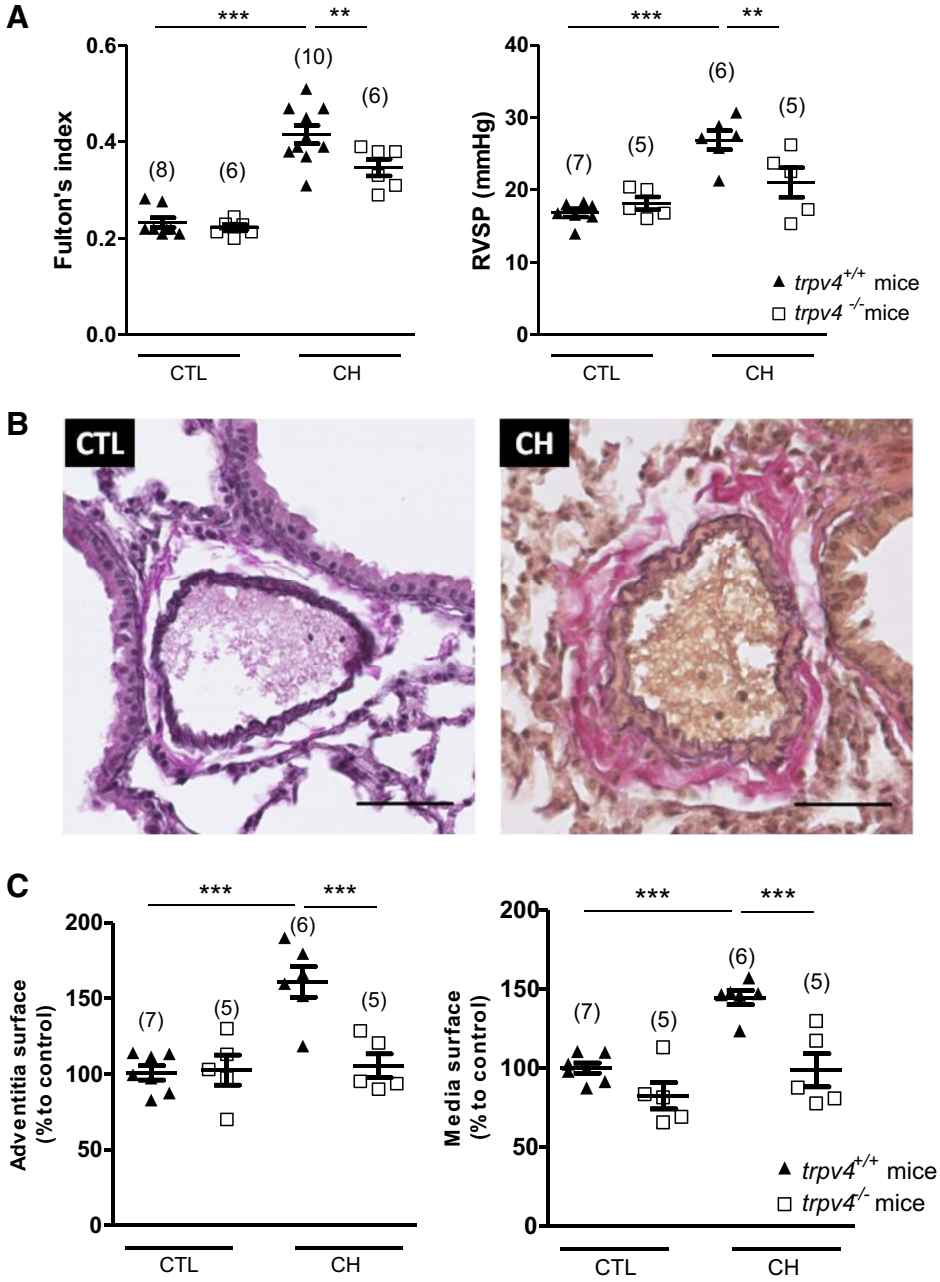

Fig. 7. Hemodynamic and pulmonary vascular morphological analyzes of the pulmonary hypertension mouse models. *A*: comparison of right ventricle hypertrophy (Fulton's index, *left*) and right ventricle systolic pressure (RVSP, *right*) for each mouse model [namely control (CTL) and chronically hypoxic (CH)] and mouse strain ($trpv4^{+/+}$ and $trpv4^{-/-}$). *B*: representative Elastica van Gieson-stained lung sections from CTL and CH $trpv4^{+/+}$ mice. Scale bar = 50 μm. *C*: comparison of adventitia (*left*) and media (*right*) surfaces for each mouse model (CTL and CH) and mouse strain ($trpv4^{+/+}$ and $trpv4^{-/-}$). The number of mice is indicated in parentheses. For morphological analysis, more than 15 lung slices were analyzed from each mouse group. Significant difference $^{**}P < 0.01$ and $^{***}P < 0.001$.

DISCUSSION

During PH, adventitia undergoes early and dramatic remodeling. These profound phenotypic changes are due, in part, to PAF activation, leading to, among others, proliferation, migration, and upregulation of extracellular matrix proteins. In the present work, using genetic (knockout mice and siRNA) and pharmacological approaches, we show, for the first time, both at cellular and integrated levels the implication of TRPV4 channels in these phenomena leading to excessive adventitial remodeling.

Indeed, since PAF are the most abundant cell type in adventitia and have been reported to be the earliest activated cells during vascular remodeling (2, 5–7, 24, 25, 41, 43), we first focused our study on this cell type. Using RT-PCR, Western blot, and calcium imaging, we demonstrated that PAF express functional TRPV4 channels, allowing intracellular Ca^{2+} increase.

Despite TRPV4 channel being clearly implicated in a variety of fibroses (pulmonary and cardiac fibrosis and scleroderma) (1, 32, 33, 40) as well as in bronchial remodeling in asthma (13), its role in adventitia remodeling occurring during PH is much more elusive. In our study, we provide a direct proof, at the cellular level, that stimulation of TRPV4 channel enhances both proliferation and migration of PAF, two crucial steps in the phenotypic change observed during development of PH. With respect to PH pathophysiology, it is noteworthy that hypoxia has also been shown to increase PAF proliferation to a greater extent than that of other pulmonary cells (24). Moreover, participation of TRPV4 channel has already been demonstrated in synovial fibroblast mitosis (17) and serotonin-

induced PASMC proliferation as the result of arachidonic acid-derived epoxyeicosatrienoic acid stimulation (10). Serotonin-induced PAF proliferation (3) might thus be related to the high circulating serotonin concentration reported in various forms of PH (16), serotonin playing a central role in the pathogenesis of pulmonary arterial remodeling. As a consequence, the pathway linking TRPV4 channel activation to PAF proliferation may represent a molecular target for the treatment of PH. Intriguingly, whereas low concentration of HC067047 (100 nM) was effective to completely abolish the GSK1016790-induced Ca^{2+} response, suggesting that this concentration is sufficient to cause complete inhibition of TRPV4 channels, this latter was ineffective for inhibiting TRPV4-induced PAF proliferation. The discrepancy in these results might have several explanations. First, it is possible that the compound presents an instability over a longer period of time, i.e., acute application in Ca^{2+} experiments (30 min) versus chronic application in proliferation assays (24 h). Alternately, as already demonstrated in a previous study (49), the inhibitory effect of HC067047 at the commonly used higher concentrations (1–5 μM) may be due to other nonspecific effects. However, in our present work, this hypothesis can be minimized as the TRPV4-dependent specific effect was verified using siRNA.

Like in PASMC (23, 30), we also showed the implication of TRPV4 in PAF migration. The increase in the $[Ca^{2+}]_i$ resulting from TRPV4-induced Ca^{2+} influx certainly plays a key role in this process, due to its role in cytoskeleton organization, such as cellular protrusion formation, focal adhesion assembly and disassembly, and cellular contractility (36). However, Ca^{2+} is probably not the only actor in the migration effect since TRPV4 channels can per se directly interact with cytoskeleton and are overexpressed in filopodial and lamellipodial structures (14, 34). Moreover, as reported in our previous study (23), TRPV1 activation produces a larger PASMC migratory response than TRPV4 one, whereas 4α-PDD induces a larger calcium response than capsaicin, showing that migration is not directly proportional to intracellular calcium increase. In this context, it would be interesting to study small G proteins such as Rho GTPase in response to channel activation, since they are known to contribute to fibroblast differentiation (52) and actin polymerization (28, 35).

Finally, TRPV4 channel activation potentiates extracellular matrix deposition by PAF as assessed by collagen type 1 and fibronectin extracellular matrix protein overexpression, thus increasing matrix stiffness. Since TRPV4 channel is notably activated by mechanical factors, this latter effect may well reinforce its role in PH. Indeed, recent studies suggest that arterial stiffening precedes PH and that hypertension, in turn, can perpetuate arterial stiffening (44). In particular, TRPV4-induced differentiation of fibroblasts into myofibroblasts is dependent on extracellular matrix stiffness in pulmonary fibrosis (32) and in cardiac remodeling following myocardial infarction (1). Moreover, fibronectin, via its extra type III domain A (ED-A) splice variant, also plays a direct positive feedback on PAF activity (8, 21, 27, 38).

Until now, it has been reported that TRPV4 is overexpressed only in the media of intrapulmonary arteries during PH development (4, 50). Using two different PH animal models (MCT and CH rats), corresponding to the first (pulmonary arterial hypertension, including idiopathic PH) and the third groups of PH (due to lung disease or chronic hypoxemia), respectively, our data indicate that TRPV4 is also overexpressed in the adventitia. Based on these findings, we can hypothesize that the variation of expression of TRPV4 channels may be an early step leading to PH. Whereas this hypothesis requires further investigation, one possible explanation could be the presence of inflammation mediators such as TNFα or TGFβ, encountered in PH, reported to increase TRPV4 expression in different types of cells such as synovial cells (20) and cardiac fibroblasts (1).

Interestingly, from a translational point of view, as already reported (50), in chronic hypoxia-induced PH, trpv4 gene deletion ($trpv4^{-/-}$ mice) significantly reduced right heart hypertrophy and RVSP increase. In contrast, in the initially controversial MCT-induced mild PH, these two parameters were not significantly decreased (data not shown), presumably due to the lesser severity of the pathology in this mouse model (39). However, despite these differences, we found a pronounced vascular remodeling of the media and adventitia in the two animal models, which was significantly reduced in $trpv4^{-/-}$ mice, thus suggesting that TRPV4 is implicated in the development of the disease.

In conclusion, this study supports the concept that PAF play a major role in hypertensive pulmonary vascular remodeling. Moreover, it addresses unresolved issues concerning the role of TRPV4 channel in PAF activation and the associated excessive adventitial remodeling observed in PH. Indeed, unravelling signaling pathways linking TRPV4 channel activation to PAF may contribute to identify innovative molecular targets for the treatment of PH.

ACKNOWLEDGMENTS

Part of the microscopy was done in the Bordeaux Imaging Center, a service unit of the CNRS-INSERM and Bordeaux University, member of the national infrastructure France BioImaging.

GRANTS

Funding for this study was provided by Université de Bordeaux and INSERM U1045.

DISCLOSURES

No conflicts of interest, financial or otherwise, are declared by the authors.

AUTHOR CONTRIBUTIONS

L.-A.C., G.C., and T.D. conceived and designed research; L.-A.C., G.C., N.T.P., M.C., P.R., A.M., and T.D. performed experiments; L.-A.C., G.C., N.T.P., M.C., P.R., A.M., and T.D. analyzed data; L.-A.C., G.C., N.T.P., and T.D. interpreted results of experiments; L.-A.C., G.C., and T.D. prepared figures; L.-A.C., G.C., and T.D. drafted manuscript; L.-A.C., G.C., A.M., C.G., P.G., R.M., J.-F.Q., J.-P.S., and T.D. edited and revised manuscript; L.-A.C., G.C., N.T.P., M.C., P.R., A.M., C.G., P.G., R.M., J.-F.Q., J.-P.S., and T.D. approved final version of manuscript.

REFERENCES

1. **Adapala RK, Thoppil RJ, Luther DJ, Paruchuri S, Meszaros JG, Chilian WM, Thodeti CK.** TRPV4 channels mediate cardiac fibroblast differentiation by integrating mechanical and soluble signals. *J Mol Cell Cardiol* 54: 45–52, 2013. doi:10.1016/j.yjmcc.2012.10.016.
2. **Chai X, Sun D, Han Q, Yi L, Wu Y, Liu X.** Hypoxia induces pulmonary arterial fibroblast proliferation, migration, differentiation and vascular remodeling via the PI3K/Akt/p70S6K signaling pathway. *Int J Mol Med* 41: 2461–2472, 2018. doi:10.3892/ijmm.2018.3462.
3. **Chen C, Han X, Fan F, Liu Y, Wang T, Wang J, Hu P, Ma A, Tian H.** Serotonin drives the activation of pulmonary artery adventitial fibroblasts and TGF-β1/Smad3-mediated fibrotic responses through 5-HT(2A)

receptors. *Mol Cell Biochem* 397: 267–276, 2014. doi:10.1007/s11010-014-2194-0.

4. **Dahan D, Ducret T, Quignard JF, Marthan R, Savineau JP, Estève E.** Implication of the ryanodine receptor in TRPV4-induced calcium response in pulmonary arterial smooth muscle cells from normoxic and chronically hypoxic rats. *Am J Physiol Lung Cell Mol Physiol* 303: L824–L833, 2012. doi:10.1152/ajplung.00244.2011.
5. **Das M, Bouchey DM, Moore MJ, Hopkins DC, Nemenoff RA, Stenmark KR.** Hypoxia-induced proliferative response of vascular adventitial fibroblasts is dependent on g protein-mediated activation of mitogen-activated protein kinases. *J Biol Chem* 276: 15631–15640, 2001. doi:10.1074/jbc.M010690200.
6. **Das M, Dempsey EC, Bouchey D, Reyland ME, Stenmark KR.** Chronic hypoxia induces exaggerated growth responses in pulmonary artery adventitial fibroblasts: potential contribution of specific protein kinase c isozymes. *Am J Respir Cell Mol Biol* 22: 15–25, 2000. doi:10.1165/ajrcmb.22.1.3536.
7. **Das M, Dempsey EC, Reeves JT, Stenmark KR.** Selective expansion of fibroblast subpopulations from pulmonary artery adventitia in response to hypoxia. *Am J Physiol Lung Cell Mol Physiol* 282: L976–L986, 2002. doi:10.1152/ajplung.00382.2001.
8. **Desmoulière A, Chaponnier C, Gabbiani G.** Tissue repair, contraction, and the myofibroblast. *Wound Repair Regen* 13: 7–12, 2005. doi:10.1111/j.1067-1927.2005.130102.x.
9. **Ducret T, El Arrouchi J, Courtois A, Quignard JF, Marthan R, Savineau JP.** Stretch-activated channels in pulmonary arterial smooth muscle cells from normoxic and chronically hypoxic rats. *Cell Calcium* 48: 251–259, 2010. doi:10.1016/j.ceca.2010.09.011.
10. **Ducret T, Guibert C, Marthan R, Savineau JP.** Serotonin-induced activation of TRPV4-like current in rat intrapulmonary arterial smooth muscle cells. *Cell Calcium* 43: 315–323, 2008. doi:10.1016/j.ceca.2007.05.018.
11. **Eul B, Rose F, Krick S, Savai R, Goyal P, Klepetko W, Grimminger F, Weissmann N, Seeger W, Hänze J.** Impact of HIF-1alpha and HIF-2alpha on proliferation and migration of human pulmonary artery fibroblasts in hypoxia. *FASEB J* 20: 163–165, 2006. doi:10.1096/fj.05-4104fje.
12. **Galiè N, Humbert M, Vachiery JL, Gibbs S, Lang I, Torbicki A, Simonneau G, Peacock A, Vonk Noordegraaf A, Beghetti M, Ghofrani A, Gomez Sanchez MA, Hansmann G, Klepetko W, Lancellotti P, Matucci M, McDonagh T, Pierard LA, Trindade PT, Zompatori M, Hoeper M.** 2015 ESC/ERS Guidelines for the diagnosis and treatment of pulmonary hypertension: The Joint Task Force for the Diagnosis and Treatment of Pulmonary Hypertension of the European Society of Cardiology (ESC) and the European Respiratory Society (ERS): Endorsed by: Association for European Paediatric and Congenital Cardiology (AEPC), International Society for Heart and Lung Transplantation (ISHLT). *Eur Respir J* 46: 903–975, 2015. doi:10.1183/13993003.01032-2015.
13. **Gombedza F, Kondeti V, Al-Azzam N, Koppes S, Duah E, Patil P, Hexter M, Phillips D, Thodeti CK, Paruchuri S.** Mechanosensitive transient receptor potential vanilloid 4 regulates *Dermatophagoides farinae*-induced airway remodeling *via* 2 distinct pathways modulating matrix synthesis and degradation. *FASEB J* 31: 1556–1570, 2017. doi:10.1096/fj.201601045R.
14. **Goswami C, Kuhn J, Heppenstall PA, Hucho T.** Importance of non-selective cation channel TRPV4 interaction with cytoskeleton and their reciprocal regulations in cultured cells. *PLoS One* 5: e11654, 2010. doi:10.1371/journal.pone.0011654.
15. **Hamanaka K, Jian MY, Weber DS, Alvarez DF, Townsley MI, Al-Mehdi AB, King JA, Liedtke W, Parker JC.** TRPV4 initiates the acute calcium-dependent permeability increase during ventilator-induced lung injury in isolated mouse lungs. *Am J Physiol Lung Cell Mol Physiol* 293: L923–L932, 2007. doi:10.1152/ajplung.00221.2007.
16. **Hervé P, Launay JM, Scrobohaci ML, Brenot F, Simonneau G, Petitpretz P, Poubeau P, Cerrina J, Duroux P, Drouet L.** Increased plasma serotonin in primary pulmonary hypertension. *Am J Med* 99: 249–254, 1995. doi:10.1016/S0002-9343(99)80156-9.
17. **Hu F, Hui Z, Wei W, Yang J, Chen Z, Guo B, Xing F, Zhang X, Pan L, Xu J.** Hypotonic stress promotes ATP release, reactive oxygen species production and cell proliferation via TRPV4 activation in rheumatoid arthritis rat synovial fibroblasts. *Biochem Biophys Res Commun* 486: 108–115, 2017. doi:10.1016/j.bbrc.2017.03.008.
18. **Humbert M, Guignabert C, Bonnet S, Dorfmüller P, Klinger JR, Nicolls MR, Olschewski AJ, Pullamsetti SS, Schermuly RT, Stenmark KR, Rabinovitch M.** Pathology and pathobiology of pulmonary hypertension: state of the art and research perspectives. *Eur Respir J* 53: 1801887, 2019. doi:10.1183/13993003.01887-2018.
19. **Jiang YL, Dai AG, Li QF, Hu RC.** Transforming growth factor-beta1 induces transdifferentiation of fibroblasts into myofibroblasts in hypoxic pulmonary vascular remodeling. *Acta Biochim Biophys Sin (Shanghai)* 38: 29–36, 2006. doi:10.1111/j.1745-7270.2006.00123.x.
20. **Kochukov MY, McNearney TA, Yin H, Zhang L, Ma F, Ponomareva L, Abshire S, Westlund KN.** Tumor necrosis factor-alpha (TNF-alpha) enhances functional thermal and chemical responses of TRP cation channels in human synoviocytes. *Mol Pain* 5: 49, 2009. doi:10.1186/1744-8069-5-49.
21. **Kohan M, Muro AF, White ES, Berkman N.** EDA-containing cellular fibronectin induces fibroblast differentiation through binding to alpha4beta7 integrin receptor and MAPK/Erk 1/2-dependent signaling. *FASEB J* 24: 4503–4512, 2010. doi:10.1096/fj.10-154435.
22. **Liedtke W, Friedman JM.** Abnormal osmotic regulation in trpv4-/- mice. *Proc Natl Acad Sci USA* 100: 13698–13703, 2003. doi:10.1073/pnas.1735416100.
23. **Martin E, Dahan D, Cardouat G, Gillibert-Duplantier J, Marthan R, Savineau JP, Ducret T.** Involvement of TRPV1 and TRPV4 channels in migration of rat pulmonary arterial smooth muscle cells. *Pflugers Arch* 464: 261–272, 2012. doi:10.1007/s00424-012-1136-5.
24. **Meyrick B, Reid L.** Hypoxia and incorporation of 3H-thymidine by cells of the rat pulmonary arteries and alveolar wall. *Am J Pathol* 96: 51–70, 1979.
25. **Meyrick BO, Reid LM.** Crotalaria-induced pulmonary hypertension. Uptake of 3H-thymidine by the cells of the pulmonary circulation and alveolar walls. *Am J Pathol* 106: 84–94, 1982.
26. **Michalick L, Erfinanda L, Weichelt U, van der Giet M, Liedtke W, Kuebler WM.** Transient receptor potential vanilloid 4 and serum glucocorticoid-regulated kinase 1 are critical mediators of lung injury in overventilated mice in vivo. *Anesthesiology* 126: 300–311, 2017. doi:10.1097/ALN.0000000000001443.
27. **Muro AF, Moretti FA, Moore BB, Yan M, Atrasz RG, Wilke CA, Flaherty KR, Martinez FJ, Tsui JL, Sheppard D, Baralle FE, Toews GB, White ES.** An essential role for fibronectin extra type III domain A in pulmonary fibrosis. *Am J Respir Crit Care Med* 177: 638–645, 2008. doi:10.1164/rccm.200708-1291OC.
28. **Nobes CD, Hall A.** Rho, rac, and cdc42 GTPases regulate the assembly of multimolecular focal complexes associated with actin stress fibers, lamellipodia, and filopodia. *Cell* 81: 53–62, 1995. doi:10.1016/0092-8674(95)90370-4.
29. **Parker JC, Hashizumi M, Kelly SV, Francis M, Mouner M, Meyer AL, Townsley MI, Wu S, Cioffi DL, Taylor MS.** TRPV4 calcium entry and surface expression attenuated by inhibition of myosin light chain kinase in rat pulmonary microvascular endothelial cells. *Physiol Rep* 1: e00121, 2013. doi:10.1002/phy2.121.
30. **Parpaite T, Cardouat G, Mauroux M, Gillibert-Duplantier J, Robillard P, Quignard JF, Marthan R, Savineau JP, Ducret T.** Effect of hypoxia on TRPV1 and TRPV4 channels in rat pulmonary arterial smooth muscle cells. *Pflugers Arch* 468: 111–130, 2016. doi:10.1007/s00424-015-1704-6.
31. **Peacock AJ, Dawes KE, Shock A, Gray AJ, Reeves JT, Laurent GJ.** Endothelin-1 and endothelin-3 induce chemotaxis and replication of pulmonary artery fibroblasts. *Am J Respir Cell Mol Biol* 7: 492–499, 1992. doi:10.1165/ajrcmb/7.5.492.
32. **Rahaman SO, Grove LM, Paruchuri S, Southern BD, Abraham S, Niese KA, Scheraga RG, Ghosh S, Thodeti CK, Zhang DX, Moran MM, Schilling WP, Tschumperlin DJ, Olman MA.** TRPV4 mediates myofibroblast differentiation and pulmonary fibrosis in mice. *J Clin Invest* 124: 5225–5238, 2014. doi:10.1172/JCI75331.
33. **Rahman M, Sun R, Mukherjee S, Nilius B, Janssen LJ.** TRPV4 Stimulation Releases ATP via Pannexin Channels in Human Pulmonary Fibroblasts. *Am J Respir Cell Mol Biol* 59: 87–95, 2018. doi:10.1165/rcmb.2017-0413OC.
34. **Ramadass R, Becker D, Jendrach M, Bereiter-Hahn J.** Spectrally and spatially resolved fluorescence lifetime imaging in living cells: TRPV4-microfilament interactions. *Arch Biochem Biophys* 463: 27–36, 2007. doi:10.1016/j.abb.2007.01.036.
35. **Ridley AJ, Paterson HF, Johnston CL, Diekmann D, Hall A.** The small GTP-binding protein rac regulates growth factor-induced membrane ruffling. *Cell* 70: 401–410, 1992. doi:10.1016/0092-8674(92)90164-8.

36. **Ridley AJ, Schwartz MA, Burridge K, Firtel RA, Ginsberg MH, Borisy G, Parsons JT, Horwitz AR.** Cell migration: integrating signals from front to back. *Science* 302: 1704–1709, 2003. doi:10.1126/science.1092053.
37. **Seghers F, Yerna X, Zanou N, Devuyst O, Vennekens R, Nilius B, Gailly P.** TRPV4 participates in pressure-induced inhibition of renin secretion by juxtaglomerular cells. *J Physiol* 594: 7327–7340, 2016. doi:10.1113/JP273595.
38. **Serini G, Bochaton-Piallat ML, Ropraz P, Geinoz A, Borsi L, Zardi L, Gabbiani G.** The fibronectin domain ED-A is crucial for myofibroblastic phenotype induction by transforming growth factor-beta1. *J Cell Biol* 142: 873–881, 1998. doi:10.1083/jcb.142.3.873.
39. **Seta F, Rahmani M, Turner PV, Funk CD.** Pulmonary oxidative stress is increased in cyclooxygenase-2 knockdown mice with mild pulmonary hypertension induced by monocrotaline. *PLoS One* 6: e23439, 2011. doi:10.1371/journal.pone.0023439.
40. **Sharma S, Goswami R, Merth M, Cohen J, Lei KY, Zhang DX, Rahaman SO.** TRPV4 ion channel is a novel regulator of dermal myofibroblast differentiation. *Am J Physiol Cell Physiol* 312: C562–C572, 2017. doi:10.1152/ajpcell.00187.2016.
41. **Stenmark KR, Davie N, Frid M, Gerasimovskaya E, Das M.** Role of the adventitia in pulmonary vascular remodeling. *Physiology (Bethesda)* 21: 134–145, 2006. doi:10.1152/physiol.00053.2005.
42. **Stenmark KR, Meyrick B, Galie N, Mooi WJ, McMurtry IF.** Animal models of pulmonary arterial hypertension: the hope for etiological discovery and pharmacological cure. *Am J Physiol Lung Cell Mol Physiol* 297: L1013–L1032, 2009. doi:10.1152/ajplung.00217.2009.
43. **Stenmark KR, Yeager ME, El Kasmi KC, Nozik-Grayck E, Gerasimovskaya EV, Li M, Riddle SR, Frid MG.** The adventitia: essential regulator of vascular wall structure and function. *Annu Rev Physiol* 75: 23–47, 2013. doi:10.1146/annurev-physiol-030212-183802.
44. **Tan W, Madhavan K, Hunter KS, Park D, Stenmark KR.** Vascular stiffening in pulmonary hypertension: cause or consequence? (2013 Grover Conference series). *Pulm Circ* 4: 560–580, 2014. doi:10.1086/677370.
45. **Thorneloe KS, Sulpizio AC, Lin Z, Figueroa DJ, Clouse AK, McCafferty GP, Chendrimada TP, Lashinger ES, Gordon E, Evans L, Misajet BA, Demarini DJ, Nation JH, Casillas LN, Marquis RW, Votta BJ, Sheardown SA, Xu X, Brooks DP, Laping NJ, Westfall TD.** N-((1S)-1-{[4-((2S)-2-{[(2,4-dichlorophenyl)sulfonyl]amino}-3-hydroxypropanoyl)-1 -piperazinyl]carbonyl}-3-methylbutyl)-1-benzothiophene-2-carboxamide (GSK1016790A), a novel and potent transient receptor potential vanilloid 4 channel agonist induces urinary bladder contraction and hyperactivity: Part I. *J Pharmacol Exp Ther* 326: 432–442, 2008. doi:10.1124/jpet.108.139295.
46. **Tofovic SP, Zhang X, Zhu H, Jackson EK, Rafikova O, Petrusevska G.** 2-Ethoxyestradiol is antimitogenic and attenuates monocrotaline-induced pulmonary hypertension and vascular remodeling. *Vascul Pharmacol* 48: 174–183, 2008. doi:10.1016/j.vph.2008.02.001.
47. **Wang D, Zhang H, Li M, Frid MG, Flockton AR, McKeon BA, Yeager ME, Fini MA, Morrell NW, Pullamsetti SS, Velegala S, Seeger W, McKinsey TA, Sucharov CC, Stenmark KR.** MicroRNA-124 controls the proliferative, migratory, and inflammatory phenotype of pulmonary vascular fibroblasts. *Circ Res* 114: 67–78, 2014. doi:10.1161/CIRCRESAHA.114.301633.
48. **White JP, Cibelli M, Urban L, Nilius B, McGeown JG, Nagy I.** TRPV4: Molecular Conductor of a Diverse Orchestra. *Physiol Rev* 96: 911–973, 2016. doi:10.1152/physrev.00016.2015.
49. **Xia Y, Fu Z, Hu J, Huang C, Paudel O, Cai S, Liedtke W, Sham JS.** TRPV4 channel contributes to serotonin-induced pulmonary vasoconstriction and the enhanced vascular reactivity in chronic hypoxic pulmonary hypertension. *Am J Physiol Cell Physiol* 305: C704–C715, 2013. doi:10.1152/ajpcell.00099.2013.
50. **Yang XR, Lin AH, Hughes JM, Flavahan NA, Cao YN, Liedtke W, Sham JS.** Upregulation of osmo-mechanosensitive TRPV4 channel facilitates chronic hypoxia-induced myogenic tone and pulmonary hypertension. *Am J Physiol Lung Cell Mol Physiol* 302: L555–L568, 2012. doi:10.1152/ajplung.00005.2011.
51. **Zhan L, Li J.** The role of TRPV4 in fibrosis. *Gene* 642: 1–8, 2018. doi:10.1016/j.gene.2017.10.067.
52. **Zhou Y, Huang X, Hecker L, Kurundkar D, Kurundkar A, Liu H, Jin TH, Desai L, Bernard K, Thannickal VJ.** Inhibition of mechanosensitive signaling in myofibroblasts ameliorates experimental pulmonary fibrosis. *J Clin Invest* 123: 1096–1108, 2013. doi:10.1172/JCI66700.